Journal of Ethnopharmacology 305 (2023) 116015

Contents lists available at ScienceDirect

Journal of Ethnopharmacology

journal homepage: www.elsevier.com/locate/jethpharm

Sophora flavescens Aiton methanol extract exerts anti-inflammatory effects via reduction of Src kinase phosphorylation

Jieun Oh [a], Seung A. Kim [a], Ki Woong Kwon [a], Se Rin Choi [b], Choong Hwan Lee [b], Mohammad Amjad Hossain [c], Eun Sil Kim [d], Changmu Kim [d], Byoung-Hee Lee [d], Sarah Lee [d,***], Jong-Hoon Kim [c,**], Jae Youl Cho [a,*]

[a] Department of Integrative Biotechnology, Sungkyunkwan University, Suwon, 16419, South Korea
[b] Department of Bioscience and Biotechnology, Konkuk University, Seoul, 05029, South Korea
[c] College of Veterinary Medicine, Chonbuk National University, Icksan, 54596, South Korea
[d] National Institute of Biological Resources, Environmental Research Complex, Incheon, 22689, South Korea

ARTICLE INFO

Keywords:
Sophora flavescens
Anti-Inflammatory effect
Src
NF-κB
IL-1β

ABSTRACT

Ethnopharmacological relevance: Sophora flavescens Aiton (Family: Leguminosae), an herbal plant, has been used in East Asian home remedies for centuries for treating ulcers, skin burns, fevers, and inflammatory disorders. In addition, the dried root of *S. flavescens* was also applied for antipyretic, analgesic, antihelmintic, and stomachic uses.

Aim of study: Nonetheless, how this plant can show various pharmacological activities including anti-inflammatory responses was not fully elucidated. In this study, therefore, we aimed to investigate the curative effects of *S. flavescens* on inflammation and its molecular mechanism.

Materials and methods: For reaching this aim, various *in vitro* and *in vivo* experimental models with LPS-treated RAW264.7 cells, HCl/EtOH-induced gastric ulcer, and LPS-triggered lung injury conditions were employed and anti-inflammatory activity of *S. flavescens* methanol extract (Sf-ME) was also tested. Fingerprinting profile of Sf-ME was identified via LC-MS analysis. Its anti-inflammatory molecular mechanism was also examined by immunoblotting analysis.

Results: Nitric oxide production and mRNA expression levels of iNOS, COX-2, IL-1β, and TNF-α were decreased. Additionally, phosphorylation of Src in the signaling cascade was decreased, and activities of the transcriptional factor NF-κB were reduced as determined by a luciferase reporter assay. Moreover, *in vivo*, gastritis and lung injury lesions were attenuated by Sf-ME.

Conclusion: Taken together, these findings suggest that Sf-ME could be a potential anti-inflammatory therapeutic agent via suppression of Src kinase activity and regulation of IL-1β secretion.

1. Introduction

Inflammation is a major defense system against life-threatening external stimuli that disrupt host homeostasis (Medzhitov, 2010). Inflammatory responses result from activation of the innate and adaptive immune systems. The innate immune system is activated by various pathogens including bacteria, viruses, and fungi (Kim et al., 2021b; Ma et al., 2021). In the initial stages of this activation, pathogen-associated molecular patterns (PAMPs) on the pathogen's surface bind to toll-like receptors (TLR) on antigen presenting cells (APCs) (Janeway and Medzhitov, 2002; Yang et al., 2021b). The type of PAMP, such as lipopolysaccharide (LPS), polyinosinic-polycytidylic acid (poly I:C) or Pam3CysSerLys4 (Pam3CSK4), binding to the APC depends on the nature of the pathogen (Mogensen, 2009). After recognition of a PAMP by

* Corresponding author.
** Corresponding author.
*** Corresponding author.
E-mail addresses: martia96@gmail.com (J. Oh), Seung-a26@naver.com (S.A. Kim), nexus0322@naver.com (K.W. Kwon), csr0701@gmail.com (S.R. Choi), chlee123@konkuk.ac.kr (C.H. Lee), mamjadh2@gmail.com (M.A. Hossain), eunsilkim@korea.kr (E.S. Kim), snubull@korea.kr (C. Kim), dpt510@korea.kr (B.-H. Lee), lsr57@korea.kr (S. Lee), jhkim1@jbnu.ac.kr (J.-H. Kim), jaecho@skku.edu (J.Y. Cho).

https://doi.org/10.1016/j.jep.2022.116015
Received 21 July 2022; Received in revised form 21 November 2022; Accepted 2 December 2022
Available online 21 December 2022

a TLR, cellular adaptor molecules couple with toll-interleukin receptor (TIR) domains allowing for activation of cytoplasmic effector molecules that create an invasion alarm (Kim et al., 2017; Wang et al., 2021). The alarm is transmitted towards the nucleus via a series of signal transducing protein phosphorylation events. This series ultimately leads to the activation of the target molecule NF-κB, a heterodimeric transcription factor that regulates a variety of cellular events. Phosphorylated NF-κB translocates into the nucleus and, to fulfill its transcription factor capacity, binds with cellular DNA (Yi et al., 2021a). The resulting gene transcription includes that of cytokines involved in combat with the pathogen and molecules involved in recruitment of inflammatory effector cells. These effector cells include natural killer (NK) cells, dendritic cells, and macrophages that engage with antigens to defend against the alien pathogen (Tan et al., 2021).

However, NF-κB activation can both rescue and endanger the host. Excessive activation of NF-κB could lead to misidentifying host cell surface molecules as pathogenic antigens. This results in a fierce attack against "self"; a variety of cytokines are released and inflammatory effector cells are activated against host cells. (Nathan and Ding, 2010). If a host fails to quell abnormal inflammation at an early stage, progression to autoimmune disease will result. This is the mechanism underlying certain cancers (Coussens and Werb, 2002), rheumatoid arthritis (Guo et al., 2018), inflammatory bowel disease (Guan, 2019), and other autoimmune diseases. Controlling NF-κB is key to achieving an appropriate inflammatory response (Yang et al., 2021a). Anti-inflammatory drugs may aid in this control. Non-steroidal anti-inflammatory drugs (NSAIDs) are one example, but these have side effects that may be severe. Less toxic alternatives are desirable, and phytochemicals derived from natural herb ingredients may be the answer.

Sophora flavescens Aiton, "Kosam" in Korea, is a species in the Leguminosae plant family. *S. flavescens* is a slow-developing evergreen that can grow up to 1.5 m (Krishna et al., 2012). The root and leaves of *S. flavescens* have been used pharmacologically as an herbal medicine around the world, especially in Korea, China, and Japan with. In traditional Chinese medicine literatures [also in State Administration of Traditional Chinese Medicine (1999), Chinese Pharmacopoeia Commission (2010)], this plant has been mentioned to use for relief of various inflammatory symptoms such as fever, dysentery, hematochezia, jaundice, oliguria, vulvar swelling, asthma, eczema, and ulcers (He et al., 2015). The Donguibogam written by Jun Heo (1610), a compilation of predominately East Asian folk medicines, describes a number of uses for the dried root and leaves of *S. flavescens* (Kim, 2019). These include antipyretic, analgesic, antihelmintic, and stomachic uses (Kim, 2019). The Donguibogam specifies the utility of this root in cases of ulcers, skin burns, fevers, and inflammatory disorders (Yoon and Kim, 2006). *S. flavescens* contains various flavonoids such as quercetin, rutin, and kushenol C; these can exert antioxidant and anti-inflammatory responses. Experimental evidence suggests that the dried root extract of *S. flavescens* can inhibit inflammatory reactions and suppress inflammatory factors, including COX-2, iNOS, NO, IL-6, and TNF-α. The effects of the aerial portion of the *S. flavescens* plant have not been reported. In this study, we examined the effects of a stem and leaf extract of *S. flavescens* on inflammation in a murine macrophage-like cell line and in acute gastritis and acute lung injury animal models.

2. Materials and methods

2.1. Materials and reagents

The methanol extract of aerial part (stems and leaves) of *S. flavescens* (Sf-ME) was supplied by the Wildlife Natural Products Bank, and the voucher specimen (No.: NIBRGR0000594812) is preserved at the herbarium of the National Institute of Biological Resources (Incheon, Korea). RAW264.7 cells (ATCC number TIB-71) and HEK293 cells (ATCC number CRL-1573) were purchased from the American Type Culture Collection (ATTC, Rockville, MD, USA). Fetal bovine serum (FBS) was purchased from Gibco (Grand Island, NY, USA). Rosewell Park Memorial Institute (RPMI) 1640 medium and Dulbecco's modified Eagle's medium (DMEM) were purchased from Cytiva (Marlborough, MA, USA). TRIzol reagent was manufactured by MRC (Cincinnati, OH, USA). For polymerase chain reactions (PCRs), both HS Taq PreMix and Probe Blue Mix Hi-ROX were procured from PCR Biosystems (Archway Road, London, UK). MTT (3-(4,5-dimethylthiazol-2-yl)-2,5-diphenyltetrazolium bromide, a tetrazole), lipopolysaccharide (LPS), dimethylsulfoxide (DMSO), and sodium dodecyl sulfate (SDS) were acquired from Sigma-Aldrich Corporation (St. Louis, MO, USA). Ethanol, methanol, and isopropanol were obtained from DAEJUNG (Seoul, Korea). Antibodies specific for β-actin and both total form and phosphorylation form of Src, Syk, IKKα/β, and IκBα were acquired from Cell Signaling Technology (Danvers, MA, USA).

2.2. Preparation of S. flavescens methanol extract, treatment of Sf-ME, and LC-MS analysis

The dried aerial part of *S. flavescens* (1 kg), was cut into pieces and extracted with 80% methanol (MeOH) for 3 h, three times in an ultrasonic apparatus. The extract was percolated through filter paper (3 mm; Whatman PLC, Kent, UK), condensed using a rotary evaporator (Büchi AG, Flawil, Switzerland) and lyophilized using a freeze dryer (Martin Christ Gefriertrocknungsanlagen, Osterode am Harz, Germany), as reported previously (Kim et al., 2021c). The powder of *S. flavescens* extract (Sf-ME) was dissolved in 80% ethanol at a concentration of 10 mg/mL for UHPLC-LTQ-Orbitrap-MS/MS analysis. Phytochemicals in Sf-ME were profiled via LC-MS Analysis. 5 μL of sample were loaded on a UHPLC-LTQ-Orbitrap-MS/MS system (Thermo, Vanquish Horizon UHPLC) with auto-sampler (Thermo, Vanquish Auto sampler). Extract was separated in a C18 column(Phenomenex KINETEX, 100 mm × 2.1 mm, 1.7 μm) and flowed with 0.1% formic acid in water and 0.1% formic acid in acetonitrile. After fractionation, each sample was ionized then detected with a mass spectrometer (Thermo, Orbitrap Velos Pro). Comparing retention time and mass fragment patterns with in-house library, references and standard compounds, each metabolite was identified.

2.3. Cell culture

Murine macrophage RAW264.7 cells were cultured at a confluency of 80–90% in 10 cm cell culture dishes using RPMI 1640 medium containing 1% penicillin, streptomycin, and 10% FBS at humidified 37 °C in a 5% CO_2 incubator. Human HEK293 cells were cultured at a density of 70–80% in 10 cm cell culture dishes using 1% penicillin, streptomycin, and 5% FBS-containing DMEM medium at humidified 37 °C in a 5% CO_2 incubator.

2.4. Nitric oxide (NO) assay

RAW264.7 cells were plated 1×10^5 cells/well in a 96 well tissue culture plate and were incubated for 18 h. Cells were pre-treated with Sf-ME (0, 25, and 50 μg/mL), L-NAME, or Bay11-7082 for 30 min; then LPS stimulation was conducted for 24 h. Supernatant from each well was collected and mixed with equivalent amounts of Griess reagent (Shu et al., 2021). Absorbance of the mixture was measured within 5 min at 540 nm. Concentration of nitric oxide (NO) was calculated by comparison with a standard curve.

2.5. MTT assay

To evaluate the cytotoxicity of Sf-ME, RAW264.7 cells and HEK293 cells were plated in 96-well plates (1×10^6 cells/mL respectively) and incubated at humidified 37 °C in a 5% CO_2 incubator. After 18 h incubation, cells were treated with Sf-ME at doses specified in the text for another 24 h. Subsequently, 10 μL of MTT solution was added, and the

Table 1
Sequences of PCR primers used in this study.

PCR type	Organism	Target	Direction	Sequence (5′ to 3′)
Semiquantitative	*Mus musculus*	IL-1β	Forward	CAGGATGAGGACATGAGCACC
Semiquantitative	*Mus musculus*	IL-1β	Reverse	CTCTGCAGACTCAAACTCCAC
Semiquantitative	*Mus musculus*	IL-6	Forward	GCCTTCTTGGGACTGATGCT
Semiquantitative	*Mus musculus*	IL-6	Reverse	TGGAAATTGGGGTAGGAAGGAC
Semiquantitative	*Mus musculus*	TNF-α	Forward	TTGACCTCAGCGCTGAGTTG
Semiquantitative	*Mus musculus*	TNF-α	Reverse	CCTGTAGCCCACGTCGTAGC
Semiquantitative	*Mus musculus*	iNOS	Forward	TGCCAGGGTCACAACTTTACA
Semiquantitative	*Mus musculus*	iNOS	Reverse	ACCCCAAGCAAGACTTGGAC
Semiquantitative	*Mus musculus*	COX-2	Forward	TCACGTGGAGTCCGCTTTAC
Semiquantitative	*Mus musculus*	COX-2	Reverse	CTTCGCAGGAAGGGGATGTT
Semiquantitative	*Mus musculus*	GAPDH	Forward	CACTCACGGCAAATTCAACGGCA
Semiquantitative	*Mus musculus*	GAPDH	Reverse	GACTCCACGACATACTCAGCAC
Real-time	*Mus musculus*	IL-1β	Forward	GTGAAATGCCACCTTTTGACAGTG
Real-time	*Mus musculus*	IL-1β	Reverse	CCTGCCTGAAGCTCTTGTTG
Real-time	*Mus musculus*	IL-6	Forward	AGCCAGAGTCCTTCAGAGAGAT
Real-time	*Mus musculus*	IL-6	Reverse	AGGAGAGCATTGGAAATTGGGG
Real-time	*Mus musculus*	TNF-α	Forward	TGCCTATGTCTCAGCCTCTT
Real-time	*Mus musculus*	TNF-α	Reverse	GAGGCCATTTGGGAACTTCT
Real-time	*Mus musculus*	iNOS	Forward	GCCACCAACAATGGCAACAT
Real-time	*Mus musculus*	iNOS	Reverse	TCGATGCACAACTGGGTGAA
Real-time	*Mus musculus*	COX-2	Forward	TTGGAGGCGAAGTGGGTTTT
Real-time	*Mus musculus*	COX-2	Reverse	TGGCTGTTTTGGTAGGCTGT
Real-time	*Mus musculus*	GAPDH	Forward	TGTGAACGGATTTGGCCGTA
Real-time	*Mus musculus*	GAPDH	Reverse	ACTGTGCCGTTGAATTTGCC

cells were incubated for 4 h (Liang et al., 2021). After incubation, the reaction was stopped by adding 15% SDS as previously reported (Lee et al., 2022).

2.6. Animals

The C57BL/6J mice and ICR mice were purchased from Orientbio (Gyeonggi-do, South Korea) and housed five mice per cage in a 12 h light/dark cycle. The care of animals was based on guidelines that were issued by the National Institute of Health for the Care and Use of Laboratory Animals (NIH Publication 80-23, revised in 1996). The study was conducted according to the guidelines that were established by the Institutional Animal Care and Use Committee (IACUC) at Sungkyunkwan University.

2.7. HCl/EtOH-induced gastritis

ICR male mice aged five weeks were housed in plastic cage for 5 days and randomly assigned to five groups (n = 5). Sf-ME and ranitidine were dissolved in 0.5% CMC and dispensed based on mouse body weight. The 150 mM HCl/60% EtOH solution was composed of 100% HPLC grade EtOH (12 mL), filtered water (8 mL), and HCl (265 μL). After removing all food and bedding for 24 h, 0.5% CMC was provided orally to the normal and negative control groups. Additionally, 50 mg/kg and 100 mg/kg Sf-ME was given to the compound treatment groups, and ranitidine 40 mg/kg was given to the positive control group. The second administration followed 8 h later, and the last oral administration was provided 16 h post-second oral injection. 8h after the last drug dosing, 150 mM HCl/60% EtOH 300 μL was administered orally to each group except the normal group; the normal group received the same volume of 0.5% CMC. One hour later, mice were sacrificed by CO_2 and stomachs were harvested (Kim et al., 2021a; Lee et al., 2020). Lesions were measured via Image J software. The approval number received for this experiment is SKKUIACUC2021-11-02-1.

2.8. LPS-induced acute lung injury

C57BL/6J male mice aged five weeks were housed in a plastic cage for five days and randomly divided into four groups (n = 5). Sf-ME and dexamethasone were dissolved in 0.5% CMC and dosed based on the body weight of the mouse. Compound-dissolved solutions were administrated three times orally. The second compound treatment was given 6 h after the first and followed 1 h later by the third treatment. All mice except normal group mice inhaled 50 μL of 5 mg/kg LPS mixture twice. After 1 h, compounds were orally delivered for the last time. Mice were euthanized 16 h after the last administration. Sacrifice and organ harvests were conducted as previously reported (Kim et al., 2021d). The approval number received for this experiment is SKKUIACUC2021-07-10-1.

2.9. RNA extraction and preparation of cDNA

RAW 264.7 cells were prepared by treating with Sf-ME for one half hour and then stimulating with LPS for 6 h. Supernatants were discarded via aspiration, and cells were frozen at −70 °C for 18 h. 300 μL of TRIzol reagent and 30 μL of 1-bromo-3-chloropropane were used for phase separation of RNA. The aqueous phase (110 μL) was cautiously collected, and the same volume of isopropanol was added for precipitation. Centrifugation of the mixture generated a small white pellet, and the precipitant was washed with 75% EtOH. Dried pellets were dissolved by DEPC-treated RNase-free water. cDNA was synthesized with 1000 ng of RNA whose A260/A280 ratio purity was between 1.8 and 2.0. Annealing oligo dT (18mer) occurred after incubation at 72 °C for 5 min in a thermal cycler. ReverAid reverse transcriptase, RiboLock RNase inhibitor, and dNTP were added up to total volume 20 μL, and cDNA synthesis was conducted per manufacturer's protocol.

2.10. RT-PCR and real-time qRT-PCR

Semi-quantitative RT-PCRs were conducted in a MiniAmp Thermal Cycler (Thermo), as reported previously (Truong et al., 2021). Electrophoresis confirmed amplification using 12 μL of PCR product in 1 x TBE agarose stained with EtBr. qRT-PCRs were conducted in a CFX96 Thermal Cycler (BioRad), as reported previously (Lee et al., 2021). 100 ng of cDNA were added to Probe Blue Mix Lo-ROX, and all the loaded samples were duplicated. The sequence of primers used for amplifications are listed in Table 1.

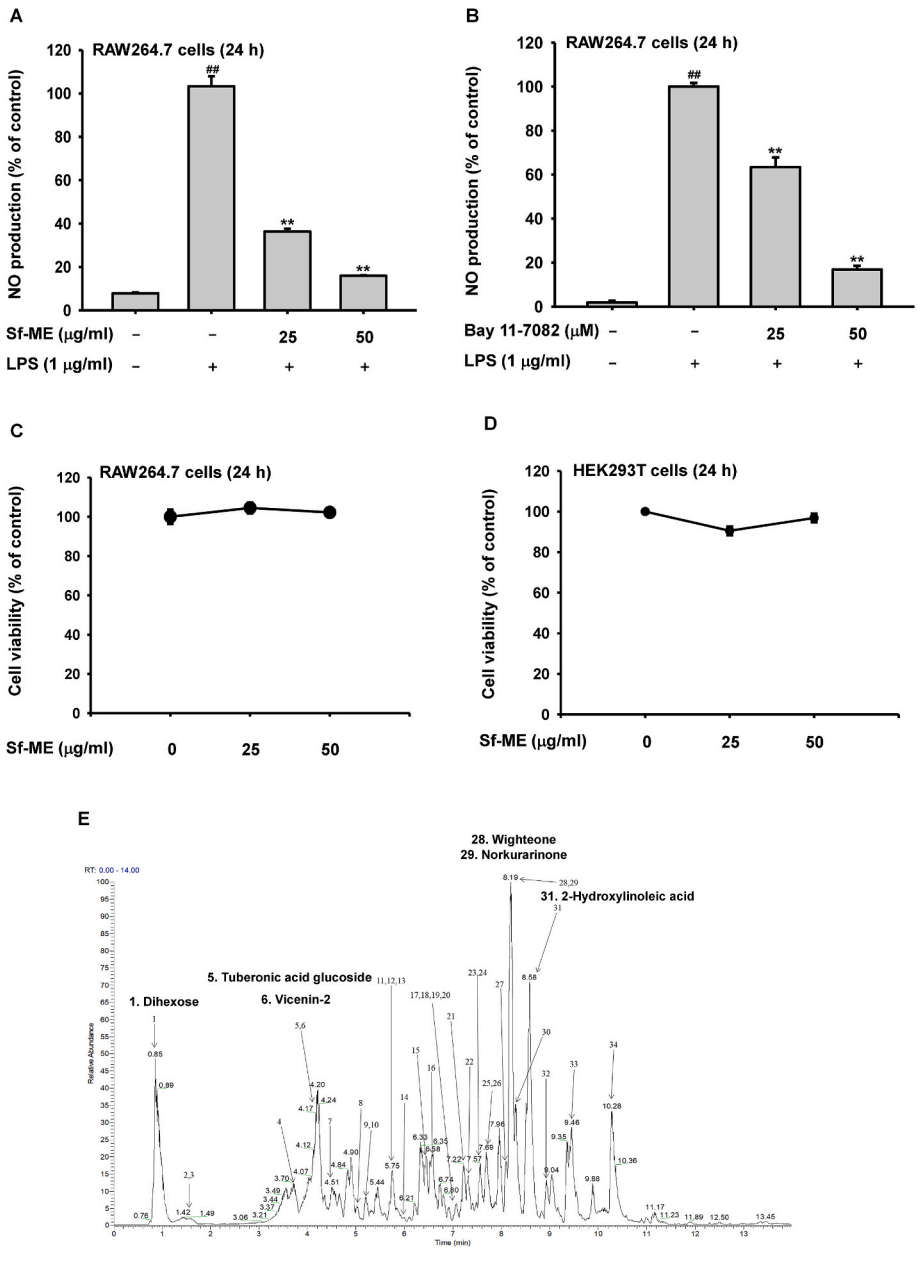

Fig. 1. Decrease of NO production in mouse-derived macrophage cell line. (**a**) The level of NO production under stimulation with LPS. (b) The ability of the IκB/IKK inhibitor to affect NO production. (c-d) RAW264.7 cell viability after Sf-ME treatment for 24 h (c) and HEK293T cell viability under the same conditions (d). (e) LC-MS/MS chromatogram analysis of Sf-ME components. All data are presented as means ± standard deviations (SDs) calculated from at least five independent samples. ##: $p < 0.01$ compared to the non-stimulated group, *: $p < 0.05$ and **: $p < 0.01$ compared to the control groups.

2.11. Luciferase reporter assay

HEK293T cells were prepared in 24-well plates. HEK293T cells were transfected with 0.8 μg each of β-galactosidase, NF-κB-Luc, and adaptor protein (Myc-MyD88 or CFP-TRIF) for 24 h. Following incubation, Sf-ME treatment occurred over an additional 24 h. Luciferase assays were performed using the Luciferase Assay System (Promega), as reported previously (Liu et al., 2021). Normalization of luciferase activity was conducted via compensation for β-galactosidase activity.

2.12. Preparing whole lysates

To acquire whole lysates, RAW264.7 cells were harvested via slight scraping and washed with ice cold PBS. After centrifugation at 3000 rpm and aspiration of PBS, fresh protease-containing ice-cold RIPA buffer (50 mM Tris-HCl, pH 7.4, 1% Nonidet P-40, 0.25% sodium deoxycholate, 150 mM NaCl, 1 mM Na_3VO_4, and 1 mM NaF) was added to lysis pellets.

2.13. Immunoblotting

Proteins in whole lysates were separated with 8–12% SDS-polyacrylamide gel electrophoresis with 100 V for 2 h. Following PAGE, proteins in the gel were transferred on PVDF membrane surfaces via a transfer sandwich kit (Bio-Rad). 1 h-long membrane incubation with 5 mL of 3% BSA dissolved in 1 x TBST was instituted to inhibit non-specific binding with primary antibodies. For detecting the specific markers Src (#2109), p-Src (Tyr416) (#2101), Syk (#2712), p-Syk (#2710), IKKα (#2682), p-IKKα/β (#2697), IκBα (#9242), p-IκBα (#9246), p50 (#12540), p65 (#8242), p-p65 (#3039) (Cell Signaling Technology), p-p50 (SC271908), and β-actin (SC4778) (Santa Cruz Biotechnology), products were used at a ratio of 1: 2500 and incubated overnight (Chow et al., 2021; Nam et al., 2021). Washing three times with 1 x TBST was followed by addition of rabbit- or mouse-derived secondary antibody (Cell Signaling Technology) for 2 h. Finally, proteins were detected with ECL solution.

2.14. In vitro ADP-Glo™ kinase assay

HEK293T cells (4.5 × 10^6 cells) plated in 100φ dishes were incubated overnight. 24 μg of Src or PI3K gene constructs were transfected and then incubated for 24 h. After incubation, cells were harvested and lysed with IP lysis buffer. 1000 μg of proteins were used for immunoprecipitation analysis. Each primary antibody which targets specifically overexpressed protein was added and incubated overnight at 4 °C. Next day, 50 μL of protein A-sepharose beads were added into the mixture and incubated for another 4 h. Beads were washed and suspended with 1x kinase buffer (25 mM Tris pH 7.5, 10 mM $MgCl_2$, 5 mM β-glycerolphosphate, 0.1 mM $NaVO_4$, and 2 mM DTT). To examine kinase inhibitory effect, we adapted ADP-Glo™ assay (Promega, Madison, WI, USA). Src kinase (as an enzyme source), p85/PI3K (as a substrate source), ATP, and Sf-ME were loaded on 384-well white plate, according to the manufacturer's instruction and previously reported (Zare et al., 2018). Each experimental group was performed in quadruplicates as expressed as % of control after set 100% with the Src activity of non-treatment group.

2.15. In vitro ubiquitination assay

HEK293T cells (3 × 10^6 cells) plated in 100φ dishes were incubated at 37 °C CO_2 chamber. Plasmid that contained Src kinase were transfected with PEI and incubated for 24 h. 100 μg/mL of Sf-ME was treated and incubated for another 24 h. After old media was aspirated, 100 μL of lysis buffer (2% SDS, 150 mM NaCl, 10 mM Tris-HCl, pH 8.0, and protease inhibitors) was added and cells were harvested with scrapper. Collected cells were boiled for 10 min and then mixed with 900 μL of dilution buffer (150 mM NaCl, 10 mM Tris-HCl, pH 8.0 2 mM EDTA, and 1% Trition). Cells were sonicated for 30 s at 30% amplitude. Following, supernatants were collected and 800 μg of proteins were prepared for immunoprecipitation. Immunoprecipitation and immunoblotting steps were preceded with previously reported protocols (Hong et al., 2022; Jiang et al., 2021).

2.16. Statistical analysis

The data are presented as the mean and standard deviation of independent replicate experiments performed with six or two technical replicates per group for statistical comparisons. Statistical comparisons were examined by a Student's *t*-test, Mann-Whitney *U* test, and one-way analysis of variance (ANOVA). A p-value <0.05 was considered statistically significant. All statistical analyses were performed using GraphPad Prism 8 software (GraphPad, San Diego, CA, USA).

3. Results

3.1. Effects of S. flavescens methanol extract (Sf-ME) on cell viability and nitric oxide (NO) production under LPS-treated conditions and phytochemical profiling of Sf-ME

To examine the effect of Sf-ME on anti-inflammatory responses, we used murine-derived macrophage-like cell line RAW264.7 and a NO production assay. NO synthesis was initiated by treating cells with LPS to stimulate TLR4. NO production was decreased to 36.3% when the dose was 25 μg/mL and 15% when the dose was 50 μg/mL (Fig. 1). We also assessed cell viability after administration of Sf-ME. A MTT assay demonstrated that 24 h treatments of RAW 264.7 cells with Sf-ME increased cell viability at both doses, 104% for 25 μg/mL and 102% for 50 μg/mL. A standard compound, BAY 11-7082, an IKK inhibitor (Lee et al., 2012), showed a significant inhibitory effect on LPS-induced NO production.

To determine which phytochemical components of Sf-ME exert the anti-inflammatory effect, we performed liquid chromatography-mass spectrometry (LC-MS/MS). The chromatogram included 34 metabolite peaks (Fig. 1E). These metabolites included daidzein, genistein, genistin, kushenol N, and kushenol D (Dong et al., 2021) as reported previously (Supplementary Table 1). However, unlike the root of *S. flavescens* used for traditional medications, the aerial portion also contained dihexose (Kumar et al., 2018), vicenin-2 (Ibrahim et al., 2015), tuberonic acid glucoside, wighteone (Wojakowska et al., 2013), norkurarinone (Dong et al., 2021), and hydroxylinoleic acid. These additional components suggest an anti-inflammatory potential.

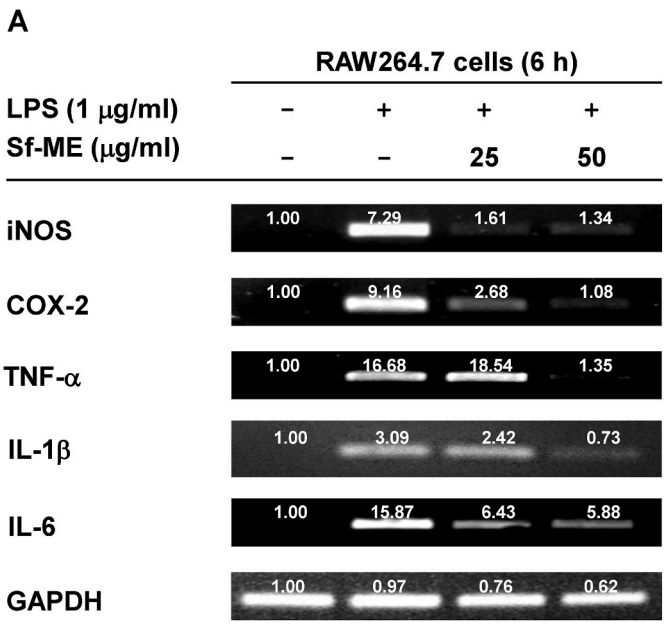

Fig. 2. Sf-ME downregulates cytokine mRNA expression under LPS stimulation. (a) Via semi-quantitative RT-PCR. Each cytokine mRNA expression level is indicated by band intensity. (b-d) Real-time qRT-PCR was conducted to quantify mRNA expression of iNOS (b), IL-6 (c), and IL-1β (d). All data are presented as means ± standard deviations (SDs) calculated from at least five independent samples. Numeric in (a) is relative intensity values, measured using ImageJ (Wayne Rasband, NIH, Bethesda, MD, USA). ##: $p < 0.01$ compared to the non-stimulated group, *: $p < 0.05$ and **: $p < 0.01$ compared to the control groups.

3.2. Decrease in cytokine mRNA expression level under LPS-treated conditions

Both real-time quantitative RT-PCR (qRT-PCR) and semi-quantitative RT-PCR (sqRT-PCR) were conducted to test for suppression of specific cytokine genes. For real-time RT-PCR, 100 ng of cDNA was used for all reactions and amplifications for 25 and 45 cycles. Via sqRT-PCR, we visualized downregulation of iNOS, COX-2, TNFα, IL-β, and IL-6 mRNA expression after Sf-ME treatment (Fig. 2a). Using real-time qRT-PCR, we confirmed gene suppression more precisely by SYBR Green signal computation as indicated in Fig. 2b-d. Each mRNA expression level was decreased in a dose-dependent manner.

3.3. Regulation of transcription factor activity

Before conducting a luciferase reporter assay, cytotoxicity of Sf-ME was determined in HEK293 cells that were used for transfection (Fig. 1d). Luciferase reporter assays were conducted to identify the transcription factors affected by Sf-ME treatment. We transfected relevant transcription factors and adaptor molecules simultaneously and evaluated activity by measuring intensity of luminescence. AP-1 and NF-κB were downregulated with both MyD88 and TRIF adaptor proteins. The greatest luminescence decrease was observed with the NF-κB and MyD88 combination. This suggested Sf-ME may exert its effects on the MyD88-mediated NF-κB, rather than AP-1, pathway (Fig. 3a-d).

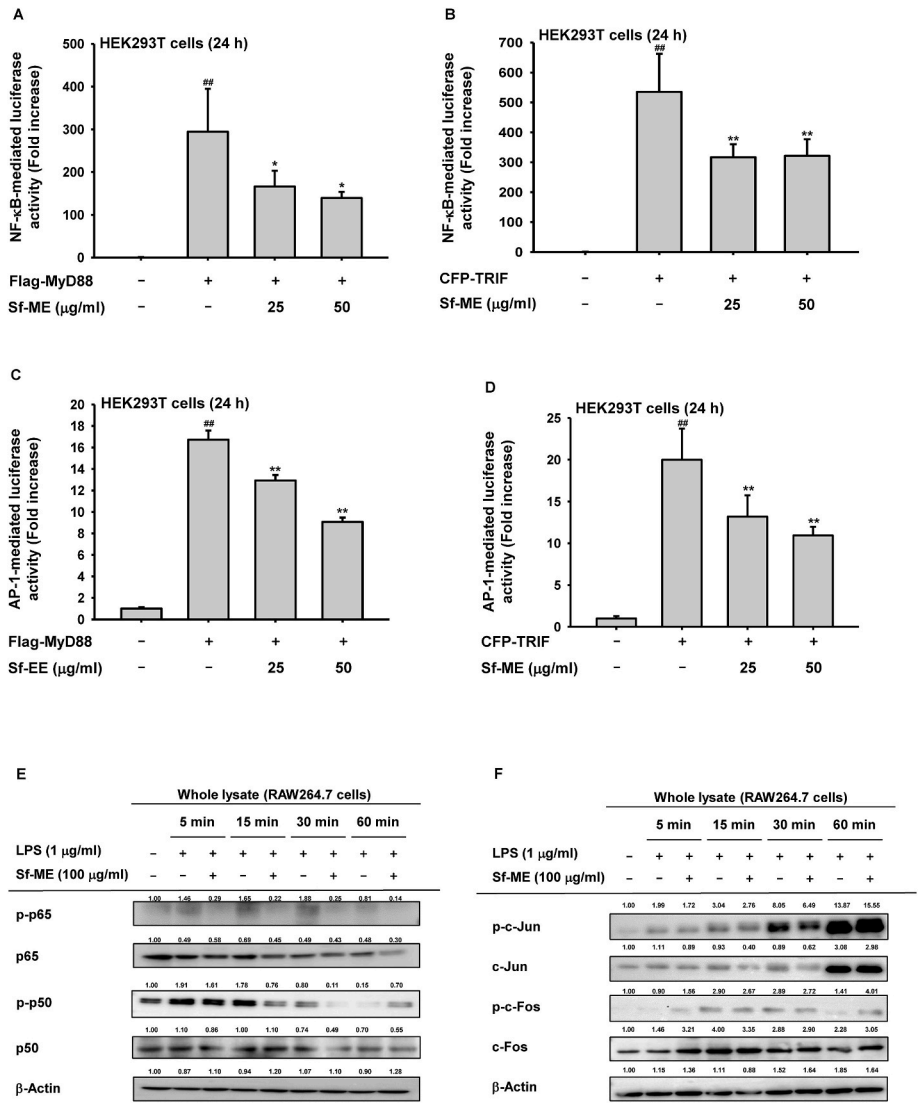

Fig. 3. Transcription factor activation is influenced by Sf-ME. (a-d) Luciferase reporter assays were conducted in HEK293T cells. NF-κB or AP-1 and adaptor molecule MyD88 or TRIF were transfected simultaneously with β-gal, and luminescence of each combination before and after treatment was measured. (e and f) The phosphorylation levels of transcription factors [NF-κB (e) and AP-1 (f)] were examined by immunoblotting analysis with whole lysates of Sf-ME-pretreated RAW264.7 cells exposed with LPS for 5, 15, 30, and 60 min. All data are presented as means ± standard deviations (SDs) calculated from at least five independent samples. Upper numeric in (e and f) is relative intensity values, measured using ImageJ (Wayne Rasband, NIH, Bethesda, MD, USA). ##: $p < 0.01$ compared to the non-stimulated group, *: $p < 0.05$ and **: $p < 0.01$ compared to the control groups.

Also, we assessed transcriptional factor phosphorylation in Sf-ME treated RAW264.7 cell lysates. As Fig. 3e shows, the phosphorylation level of p65 was reduced from 5 to 50 min during Sf-ME- treated conditions, while phospho-p50 levels were strikingly downregulated at 15 and 30 min in Sf-ME-treated groups (Fig. 3e). Meanwhile, since AP-1-mediated luciferase activity was also reduced by this extract (Fig. 3c and d), we also examined whether Sf-ME can also affect the phosphorylation patterns of AP-1 transcription factors using immunoblotting analysis. Unfortunately, the phosphorylation levels of c-Jun and c-Fos was not strikingly altered by Sf-ME, when the intensity was calculated with their total forms. This result seems to imply that downregulation of AP-1 activity by Sf-ME is not a major outcome in Sf-ME-mediated anti-inflammatory action.

3.4. Src phosphorylation regulation in signaling cascade

One of the important characteristics of innate immunity is the TLR signal transduction cascade from TLR to transcription factor. To determine time-dependent changes in signal amplification, we performed cell lysate immunoblotting at different time points, 5, 15, 30, and 60 min, to test late signaling activities and at 2, 3, and 5 min to test the early cascade activities.

Kinases comprising the signaling cascade regulating NF-κB activation, including IKK and IKBα, were tested for activation under Sf-ME treatment conditions. This approach revealed that the phospho-IκBα level was reduced at 5 min (weakly), and 30 and 60 min (strongly), as shown in the case of p-IKKα/β level (Fig. 4a). Since early state of phosphorylation was reported to be regulated by Src and Syk (Kim et al., 2021a, 2021c), we also confirmed whether Sf-ME can reduce the phosphorylation of these enzymes with whole cell lysates of Sf-ME-pretreated RAW264.7 cells exposed with LPS for 2, 3, and 5 min. As Fig. 4B show, Src phosphorylation was found to be reduced by Sf-ME at 2 and 3 min. These findings indicate that Src may be a target protein of Sf-ME in the NF-κB pathway. To ensure this possibility, we directly tested inhibitory activity of Sf-ME on Src activity using kinase assay conditions. Expectedly, Sf-ME strongly suppressed Src kinase activity up to 70% (Fig. 4c).

Since Sf-ME reduced the level of post-translational modification of Src (eg., phosphorylation), we also conducted to check whether ubiquitination level of Src can be also controlled by this extract using whole cell lysates prepared with Src-overexpressed HEK293 cells. As Fig. 4d shows, there was no striking difference between treatment and non-treatment of Sf-ME, implying that Src degradation was not regulated by this extract.

3.5. Anti-inflammatory effect of Sf-ME in vivo disease models

Acute lung injury was induced via nasal administration of 5 mg/kg

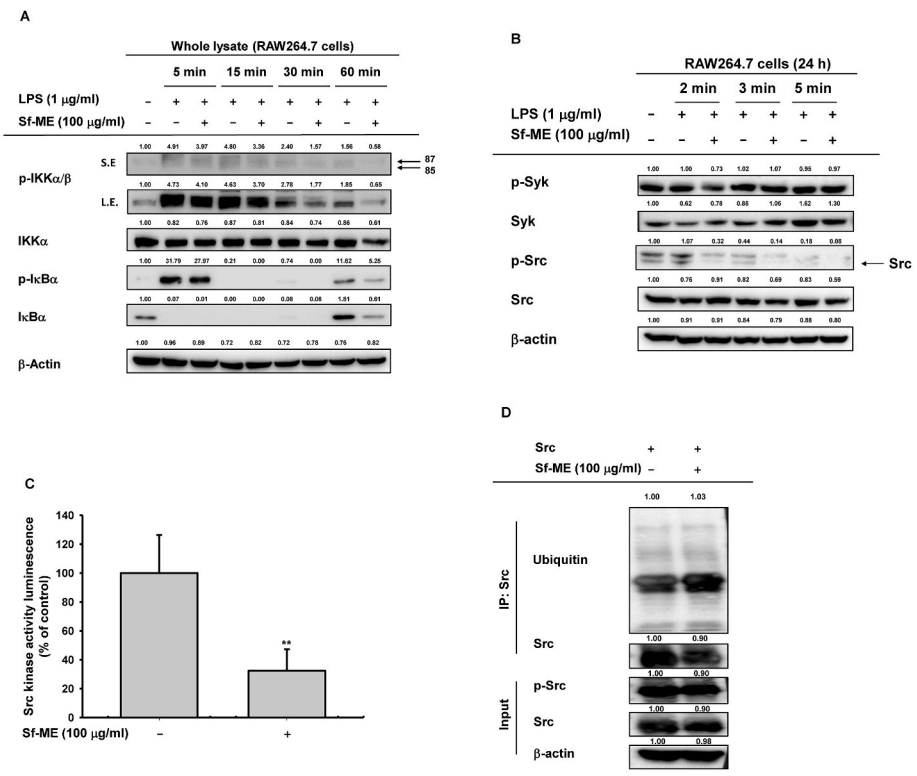

Fig. 4. Phosphorylation in the NF-κB-related signaling cascade was reduced by Sf-ME treatment. (a) Downstream proteins in the signaling cascade were analyzed with whole cell lysates. Each cell was harvested at 5, 15, 30, and 60 min after LPS stimulation. (b) Short-term responses were analyzed to determine early signaling events. All data are presented as means ± standard deviations (SDs) calculated from at least five independent samples. (c) Kinase activity of Src under Sf-ME-treated conditions was examined by ADP-Glo™ assay. S.E: Short exposure, L.E: long exposure. (d) Regulatory effect of Sf-ME on Src ubiquitination pattern was examined by ubiquitination experiment, immunoprecipitation, and immunoblotting analyses. Upper numeric in (a, b, and d) is relative intensity values, measured using ImageJ (Wayne Rasband, NIH, Bethesda, MD, USA). ##: $p < 0.01$ compared to the non-stimulated group, *: $p < 0.05$ and **: $p < 0.01$ compared to the control groups.

LPS solution, and the anti-inflammatory effect of Sf-ME was evaluated by histological and mRNA expression data (Fig. 5a-b). H&E staining revealed that alveolar damage was reduced in the Sf-ME pre-treatment group. Also, IL-1β mRNA expression was suppressed with Sf-ME inhalation treatment. Sf-ME showed a similar preventive effect on acute gastritis. Blood spot areas in the stomach indicative of mucosal membrane damage extent were reduced with administration of Sf-ME compared to the negative control group (Fig. 5c). A suppressive effect of Sf-ME on cytokine gene expression was confirmed with real-time qRT-PCR as shown in Fig. 5d. Also, phosphorylation of the two dimers, p50 and p65, was reduced.

4. Discussion

Sophora genus members, comprised of over 70 species, are indigenous to Asia, Oceania, and the Pacific Islands (Abd-Alla et al., 2021). Among the *Sophora* genera, *S. flavescens* has been used in folk medicine, especially its root. The root of *S. flavescens* has been brewed as a tea, but the bitter taste is a hurdle to its use as a medicine. *S. flavescens* powder has been used for treating urticaria in Korea, and this is documented in the Donguibogam (Heo, 1969). A variety of secondary metabolites including flavonoids, alkaloids, and other components have been identified in *S. flavescens* roots. Among these compounds, the kushenol compounds have anti-inflammatory effects. Our LC-MS/MS analysis determined that the aerial part of *S. flavescens* also has kushenol N and kushenol D. In addition, dihexoses, vicenin-2, genistin, genistein, wighteone, and tuberonic acid glucoside were detected as major components (Supplementary Table 1). Based on ethnopharmacological knowledge and the LC-MS/MS results (Fig. 1e), we tested the anti-inflammatory effects of Sf-ME.

We demonstrated for the first time that Sf-ME reduced NO secretion which was activated by TLR4 stimulation with LPS. NO is a signal carrier under inflammatory conditions; NO production is intimately involved in the pathogenesis of inflammation (Rahmawati et al., 2021). NO inhibition efficacy of Sf-ME was compared with that of BAY 11-7082, the kinase inhibitor. Suppressed iNOS mRNA expression level was evidence of Sf-ME's NO inhibitory ability as shown in Fig. 1A. Moreover, attenuation of expression of various cytokine genes including those for COX-2, TNF-α, and the interleukins indicate anti-inflammatory effects of Sf-ME.

Moreover, activity of transcription factors that direct inflammation responses was downregulated. Luciferase reporter assays demonstrated functional activity of the adaptor molecules that interact with the cytoplasmic domain of TLR4 and the inactivation of major transcription factors that direct inflammation responses (Yang et al., 2020a, 2020b). Compared to the non-treatment group, both AP-1 and NF-κB pathways were deactivated by Sf-ME treatment. Since AP-1 and NF-κB families are core components of the transcription factor network (Kim et al., 2021d), these results suggest that Sf-ME affects inflammation control at the cellular level. Phosphorylation levels of kinase proteins were assessed by immunoblotting. Signal cascades that are induced by activation of classical immunoreceptors such as TLRs, were tightly regulated by Sf-ME. The Src family of protein tyrosine kinases play key roles in signal transduction regulation (Parsons and Parsons, 2004). With a diverse set of cell surface receptors, Src is a component of multiple molecular operations that couple receptors (Yi et al., 2021b). Regulating Src kinase activity, as assessed by ADP-GloTM kinase assay (Fig. 4c), can affect fundamental cellular processes like cell growth, cell differentiation, cell migration, and cell survival (Lowell, 2011). Sf-ME's impacts on Src could have a wide range of effects on basic cellular mechanisms. Future research should focus on Sf-ME's target binding site in Src domains and an overexpression of candidate target gene experiments.

Sf-ME not only prevented phosphorylation/kinase activity of Src, but also IKK. The IKK kinase complex is composed of two kinases, IKKα and IKKβ, and a regulatory subunit NEMO/IKKγ. Activation of the IKK kinase subunit ultimately induces nuclear translocation of NF-κB heterodimers (Israel, 2010). With Sf-ME treatment, phosphorylation of IKK was downregulated; this can influence NF-κB heterodimeric activity as shown as Fig. 3e.

Effects of Sf-ME *in vivo* were examined in two animal disease models: an acute gastritis model and an acute lung injury (ALI) model (Kim et al., 2021a, 2021d). At the point of tissue damage, Sf-ME demonstrated

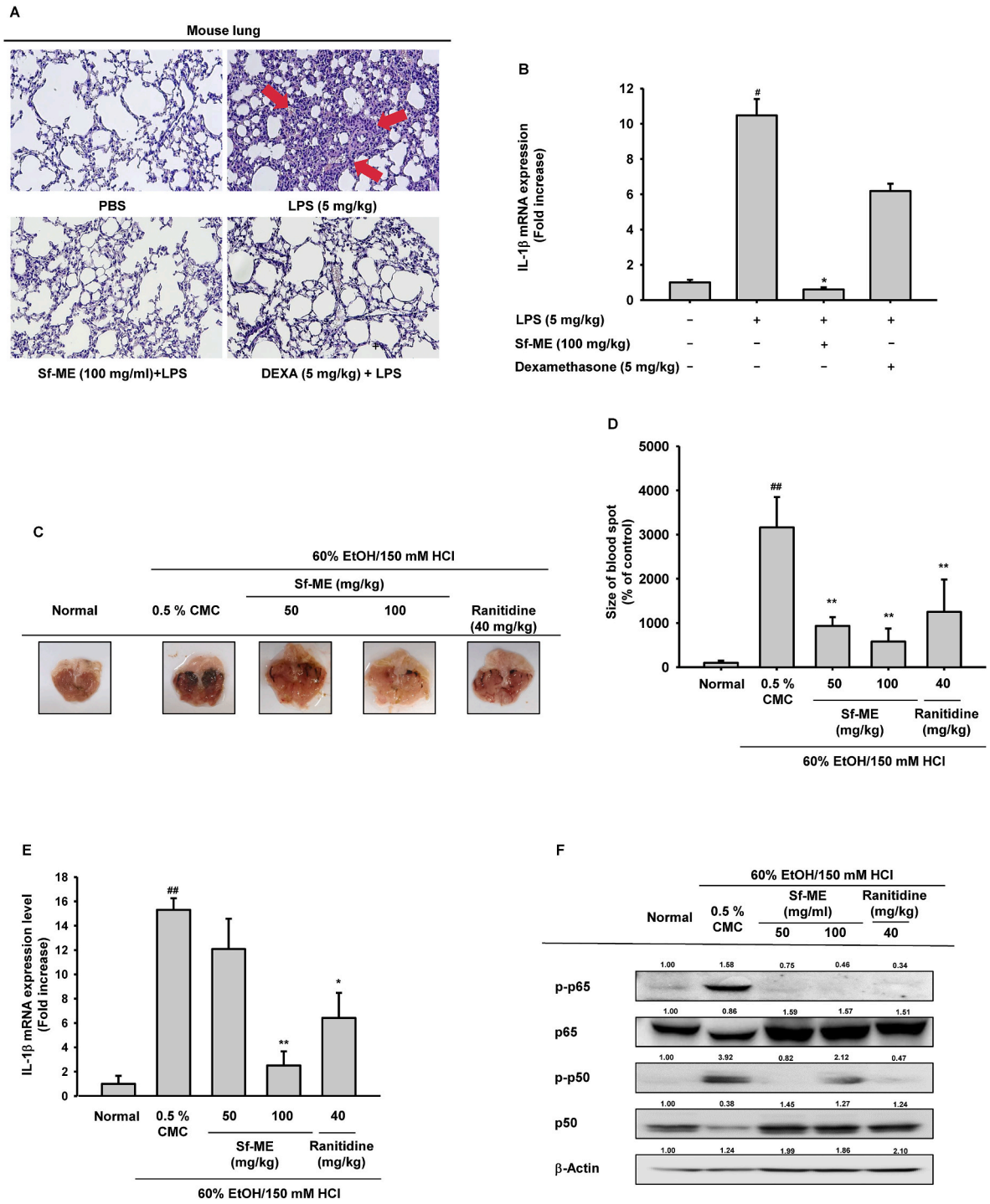

Fig. 5. Effect of Sf-ME in the *in vivo* experiments. (a) Sf-ME showed preventive effects on lung tissue damage after acute lung injury. (b) mRNA expression level of IL-1β was suppressed under Sf-ME treatment conditions. (c) Stomach images after acute gastritis induction. (d) Blood spot regions were measured via Image J software. (e) mRNA expression was quantified with real-time qRT-PCR of stomach tissue. (f) Stomach tissue lysates were immunoblotted with p50, p65, phospho-p50, and phospho-p65 antibodies. All data are presented as means ± standard deviations (SDs) calculated from at least five independent samples. Upper numeric in (f) is relative intensity values, measured using ImageJ (Wayne Rasband, NIH, Bethesda, MD, USA). Arrows in (a) indicate alveolar damages. ##: $p < 0.01$ compared to the non-stimulated group, *: $p < 0.05$ and **: $p < 0.01$ compared to the control groups.

damage prevention in both conditions. In the ALI model, fibrosis of alveoli was reduced as shown in Fig. 5a, and the size of blood spots in the stomach wall was decreased in the gastritis model.

Moreover, IL-1β mRNA expression level was downregulated in the animal disease models. IL-1β is one of the major pro-inflammatory cytokines produced by cells of the innate immune system (Dinarello, 2018). The IL-1 family has two subtypes, IL-1α and IL-1β, which can exert pleiotropic effects on a variety of cell types (Kaneko et al., 2019). Via binding with IL-1RI, IL-1 receptor accessory protein is recruited for assembly of a high-affinity binding complex. Since IL-1β maintains homeostasis, overproduction of IL-1β would be implicated in disruption of the host's immune system equilibrium. Blocking IL-1β is a standard approach for treating inflammatory syndromes; therefore, the IL-1β suppressive ability of Sf-ME suggests its potential to be an herbal

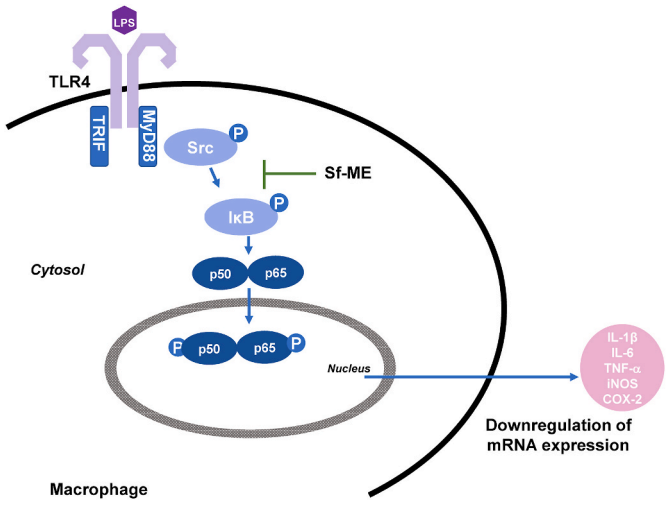

Fig. 6. Putative mechanism of Sf-ME's anti-inflammatory effect.

treatment for a variety of inflammatory diseases.

5. Conclusions

We have demonstrated that Sf-ME can suppress acute inflammation via attenuation of Src kinase phosphorylation and reduction of IL-1β mRNA expression as summarized in Fig. 6. These findings indicate that Sf-ME can be an herbal medicine for regulating inflammation symptoms. Sf-ME requires further testing prior to pharmacological use. Toxicities or any probabilities for side effects need to be quantified. Findings related to Sf-ME's mechanism of action can increase our national ethnopharmacological knowledge and improve our understanding of inflammation downregulation.

Funding

This research was supported by a grant from the National Institute of Biological Resources (NIBR) funded by the Ministry of Environment (MOE) of the Republic of Korea (Grant No.: NIBR202121102 and NIBR202220102).

CRediT authorship contribution statement

Jieun Oh: conceived and designed the experiments, Formal analysis, performed the experiments, wrote the manuscript. **Seung A. Kim:** performed the experiments. **Ki Woong Kwon:** performed the experiments. **Se Rin Choi:** performed the experiments, All authors have read and agreed to the published version of the manuscript. **Choong Hwan Lee:** Formal analysis. **Mohammad Amjad Hossain:** performed the experiments. **Eun Sil Kim:** Formal analysis, wrote the manuscript. **Changmu Kim:** Formal analysis. **Byoung-Hee Lee:** Formal analysis. **Sarah Lee:** conceived and designed the experiments, Formal analysis, wrote the manuscript. **Jong-Hoon Kim:** conceived and designed the experiments, Formal analysis, wrote the manuscript. **Jae Youl Cho:** conceived and designed the experiments, Formal analysis, wrote the manuscript.

Declaration of competing interest

The authors declare no conflict of interest.

Data availability

Data will be made available on request.

Acknowledgments

Not applicable.

Appendix A. Supplementary data

Supplementary data to this article can be found online at https://doi.org/10.1016/j.jep.2022.116015.

Abbreviations

Sf-ME	*Sophora flavescens* methanol extract
TRIF	TIR-domain-containing adaptor protein inducing interferon-β
LPS	lipopolysaccharide
PRRs	pattern recognition receptors
COX-2	cyclooxygenase-2
TLR4	toll-like receptor 4
NO	nitric oxide
iNOS	inducible nitric oxide synthase
IL-1β	interleukin 1 beta
MyD88	myeloid differentiation factor 88
NF-κB	nuclear factor-κB
PEI	polyethylene imidazole
IL-6	interleukin 6
CMC	carboxymethylcellulose

References

Abd-Alla, H.I., Souguir, D., Radwan, M.O., 2021. Genus Sophora: a comprehensive review on secondary chemical metabolites and their biological aspects from past achievements to future perspectives. Arch Pharm. Res. (Seoul) 44, 903–986.
Chow, P.M., Chang, Y.W., Kuo, K.L., Lin, W.C., Liu, S.H., Huang, K.H., 2021. CDK7 inhibition by THZ1 suppresses cancer stemness in both chemonaive and chemoresistant urothelial carcinoma via the hedgehog signaling pathway. Cancer Lett. 507, 70–79.
Coussens, L.M., Werb, Z., 2002. Inflammation and cancer. Nature 420, 860–867.
Dinarello, C.A., 2018. Overview of the IL-1 family in innate inflammation and acquired immunity. Immunol. Rev. 281, 8–27.
Dong, Y., Jia, G., Hu, J., Liu, H., Wu, T., Yang, S., Li, Y., Cai, T., 2021. Determination of alkaloids and flavonoids in Sophora flavescens by UHPLC-Q-TOF/MS. J. Anal. Method. Chem. 2021, 9915027.
Guan, Q., 2019. A comprehensive review and update on the pathogenesis of inflammatory bowel disease. J. Immunol. Res. 2019, 7247238.
Guo, Q., Wang, Y., Xu, D., Nossent, J., Pavlos, N.J., Xu, J., 2018. Rheumatoid arthritis: pathological mechanisms and modern pharmacologic therapies. Bone Res. 6, 15.
He, X., Fang, J., Huang, L., Wang, J., Huang, X., 2015. Sophora flavescens Ait.: traditional usage, phytochemistry and pharmacology of an important traditional Chinese medicine. J. Ethnopharmacol. 172, 10–29.
Heo, J., 1969. Gukyeok Jeungbo Dongeui Bogam. Namsandang, Seoul.
Hong, Y.H., Aziz, N., Park, J.G., Lee, D., Kim, J.K., Kim, S.A., Choi, W., Lee, C.Y., Lee, H. P., Huyen Trang, H.T., Kim, H.G., Jeon, Y.J., Kim, B., Kim, Y., Kim, K.H., Yoo, B.C., Han, J.W., Parameswaran, N., Kim, J.H., Hur, H., Cho, J.Y., 2022. The EEF1AKMT3/MAP2K7/TP53 axis suppresses tumor invasiveness and metastasis in gastric cancer. Cancer Lett. 544, 215803.
Ibrahim, R.M., El-Halawany, A.M., Saleh, D.O., Naggar, E.M.B.E., El-Shabrawy, A.E.-R. O., El-Hawary, S.S., 2015. HPLC-DAD-MS/MS profiling of phenolics from Securigera securidaca flowers and its anti-hyperglycemic and anti-hyperlipidemic activities. Revista Brasileira de Farmacognosia 25, 134–141.
Israel, A., 2010. The IKK complex, a central regulator of NF-kappaB activation. Cold Spring Harbor Perspect. Biol. 2, a000158.
Janeway Jr., C.A., Medzhitov, R., 2002. Innate immune recognition. Annu. Rev. Immunol. 20, 197–216.
Jiang, L., Chen, Y., Min, G., Wang, J., Chen, W., Wang, H., Wang, X., Yao, N., 2021. Bcl2-associated athanogene 4 promotes the invasion and metastasis of gastric cancer cells by activating the PI3K/AKT/NF-kappaB/ZEB1 axis. Cancer Lett. 520, 409–421.
Kaneko, N., Kurata, M., Yamamoto, T., Morikawa, S., Masumoto, J., 2019. The role of interleukin-1 in general pathology. Inflamm. Regen. 39, 12.
Kim, J.H., Yi, Y.S., Kim, M.Y., Cho, J.Y., 2017. Role of ginsenosides, the main active components of Panax ginseng, in inflammatory responses and diseases. J. Ginseng. Res. 41, 435–443.
Kim, J.K., Choi, E., Hong, Y.H., Kim, H., Jang, Y.J., Lee, J.S., Choung, E.S., Woo, B.Y., Hong, Y.D., Lee, S., Lee, B.H., Bach, T.T., Kim, J.H., Kim, J.H., Cho, J.Y., 2021a. Syk/NF-kappaB-targeted anti-inflammatory activity of Melicope accedens (Blume) T.G. Hartley methanol extract. J. Ethnopharmacol. 271, 113887.
Kim, J.K., Shin, K.K., Kim, H., Hong, Y.H., Choi, W., Kwak, Y.S., Han, C.K., Hyun, S.H., Cho, J.Y., 2021b. Korean Red Ginseng exerts anti-inflammatory and autophagy-promoting activities in aged mice. J. Ginseng. Res. 45, 717–725.

Kim, S.A., Lee, C.Y., Mitra, A., Kim, H., Woo, B.Y., Hong, Y.D., Noh, J.K., Yi, D.K., Kim, H. G., Cho, J.Y., 2021c. Anti-inflammatory effects of Huberia peruviana Cogn. Methanol extract by inhibiting Src activity in the NF-kappaB pathway. Plants 10.
Kim, S.A., Oh, J., Choi, S.R., Lee, C.H., Lee, B.H., Lee, M.N., Hossain, M.A., Kim, J.H., Lee, S., Cho, J.Y., 2021d. Anti-gastritis and anti-lung injury effects of pine tree ethanol extract targeting both NF-kappaB and AP-1 pathways. Molecules 26.
Kim, T., 2019. Text and practice in East Asian medicine: the structure of East Asian medical knowledge examined by Donguibogam currents in contemporary South Korea. Uisahak 28, 591–620.
Krishna, P.M., Knv, R., S, S., Banji, D., 2012. A review on phytochemical, ethnomedical and pharmacological studies on genus Sophora. Fabaceae. Revista Brasileira de Farmacognosia 22, 1145–1154.
Kumar, S., Sephuhle, N., Bouic, P.J., Rosenkranz, B., 2018. HPLC/LC-MS guided phytochemical and in vitro screening of Astragalus membranaceus (Fabaceae), and prediction of possible interactions with CYP2B6. J. Herb. Med. 14, 35–47.
Lee, H.P., Kim, D.S., Park, S.H., Shin, C.Y., Woo, J.J., Kim, J.W., An, R.-B., Lee, C., Cho, J. Y., 2022. Antioxidant capacity of Potentilla paradoxa Nutt. And its beneficial effects related to anti-aging in HaCaT and B16F10 cells. Plants 11, 873.
Lee, J., Rhee, M.H., Kim, E., Cho, J.Y., 2012. BAY 11-7082 is a broad-spectrum inhibitor with anti-inflammatory activity against multiple targets. Mediat. Inflamm., 416036, 2012.
Lee, J.O., Hwang, S.H., Shen, T., Kim, J.H., You, L., Hu, W., Cho, J.Y., 2021. Enhancement of skin barrier and hydration-related molecules by protopanaxatriol in human keratinocytes. J. Ginseng. Res. 45, 354–360.
Lee, J.O., Kim, J.H., Kim, S., Kim, M.Y., Hong, Y.H., Kim, H.G., Cho, J.Y., 2020. Gastroprotective effects of the nonsaponin fraction of Korean Red Ginseng through cyclooxygenase-1 upregulation. J. Ginseng. Res. 44, 655–663.
Liang, H., Li, T., Fang, X., Xing, Z., Zhang, S., Shi, L., Li, W., Guo, L., Kuang, C., Liu, H., Yang, Q., 2021. IDO1/TDO dual inhibitor RY103 targets Kyn-AhR pathway and exhibits preclinical efficacy on pancreatic cancer. Cancer Lett. 522, 32–43.
Liu, M., Qin, Y., Hu, Q., Liu, W., Ji, S., Xu, W., Fan, G., Ye, Z., Zhang, Z., Xu, X., Yu, X., Zhuo, Q., 2021. SETD8 potentiates constitutive ERK1/2 activation via epigenetically silencing DUSP10 expression in pancreatic cancer. Cancer Lett. 499, 265–278.
Lowell, C.A., 2011. Src-family and Syk kinases in activating and inhibitory pathways in innate immune cells: signaling cross talk. Cold Spring Harbor Perspect. Biol. 3.
Ma, D., Zhan, D., Fu, Y., Wei, S., Lal, B., Wang, J., Li, Y., Lopez-Bertoni, H., Yalcin, F., Dzaye, O., Eberhart, C.G., Laterra, J., Wilson, M.A., Ying, M., Xia, S., 2021. Mutant IDH1 promotes phagocytic function of microglia/macrophages in gliomas by downregulating ICAM1. Cancer Lett. 517, 35–45.
Medzhitov, R., 2010. Inflammation 2010: new adventures of an old flame. Cell 140, 771–776.
Mogensen, T.H., 2009. Pathogen recognition and inflammatory signaling in innate immune defenses. Clin. Microbiol. Rev. 22, 240–273 (Table of Contents).
Nam, S.M., Choi, J.H., Choi, S.H., Cho, H.J., Cho, Y.J., Rhim, H., Kim, H.C., Cho, I.H., Kim, D.G., Nah, S.Y., 2021. Ginseng gintonin alleviates neurological symptoms in the G93A-SOD1 transgenic mouse model of amyotrophic lateral sclerosis through lysophosphatidic acid 1 receptor. J. Ginseng. Res. 45, 390–400.
Nathan, C., Ding, A., 2010. Nonresolving inflammation. Cell 140, 871–882.
Parsons, S.J., Parsons, J.T., 2004. Src family kinases, key regulators of signal transduction. Oncogene 23, 7906–7909.
Rahmawati, L., Park, S.H., Kim, D.S., Lee, H.P., Aziz, N., Lee, C.Y., Kim, S.A., Jang, S.G., Kim, D.S., Cho, J.Y., 2021. Anti-inflammatory activities of the ethanol extract of Prasiola japonica, an edible freshwater green algae, and its various solvent fractions in LPS-induced macrophages and carrageenan-induced paw edema via the AP-1 pathway. Molecules 27.
Shu, P.P., Li, L.X., He, Q.M., Pan, J., Li, X.L., Zhu, M., Yang, Y., Qu, Y., 2021. Identification and quantification of oleanane triterpenoid saponins and potential analgesic and anti-inflammatory activities from the roots and rhizomes of Panax stipuleanatus. J. Ginseng. Res. 45, 305–315.
Tan, Y.N., Li, Y.P., Huang, J.D., Luo, M., Li, S.S., Lee, A.W., Hu, F.Q., Guan, X.Y., 2021. Thermal-sensitive lipid nanoparticles potentiate anti-PD therapy through enhancing drug penetration and T lymphocytes infiltration in metastatic tumor. Cancer Lett. 522, 238–254.
Truong, V.L., Keum, Y.S., Jeong, W.S., 2021. Red ginseng oil promotes hair growth and protects skin against UVC radiation. J. Ginseng. Res. 45, 498–509.
Wang, Y.Y., Hung, A.C., Lo, S., Yuan, S.F., 2021. Adipocytokines visfatin and resistin in breast cancer: clinical relevance, biological mechanisms, and therapeutic potential. Cancer Lett. 498, 229–239.
Wojakowska, A., Piasecka, A., Garcia-Lopez, P.M., Zamora-Natera, F., Krajewski, P., Marczak, L., Kachlicki, P., Stobiecki, M., 2013. Structural analysis and profiling of phenolic secondary metabolites of Mexican lupine species using LC-MS techniques. Phytochemistry 92, 71–86.
Yang, F., Duan, M., Zheng, F., Yu, L., Wang, Y., Wang, G., Lin, J., Han, S., Gan, D., Meng, Z., Zhu, S., 2021a. Fas signaling in adipocytes promotes low-grade inflammation and lung metastasis of colorectal cancer through interaction with Bmx. Cancer Lett. 522, 93–104.
Yang, J., Li, Y., Sun, Z., Zhan, H., 2021b. Macrophages in pancreatic cancer: an immunometabolic perspective. Cancer Lett. 498, 188–200.
Yang, W.S., Kim, H.G., Kim, E., Han, S.Y., Aziz, N., Yi, Y.S., Kim, S., Lee, Y., Yoo, B.C., Han, J.W., Parameswaran, N., Kim, J.H., Cho, J.Y., 2020a. Isoprenylcysteine carboxyl methyltransferase and its substrate ras are critical players regulating TLR-mediated inflammatory responses. Cells 9.
Yang, W.S., Kim, H.G., Lee, Y., Yoon, K., Kim, S., Kim, J.H., Cho, J.Y., 2020b. Isoprenylcysteine carboxyl methyltransferase inhibitors exerts anti-inflammatory activity. Biochem. Pharmacol. 182, 114219.
Yi, H., Liang, L., Wang, H., Luo, S., Hu, L., Wang, Y., Shen, X., Xiao, L., Zhang, Y., Peng, H., Dai, C., Yuan, L., Li, R., Gong, F., Li, Z., Ye, M., Liu, J., Zhou, H., Zhang, J., Xiao, X., 2021a. Albendazole inhibits NF-kappaB signaling pathway to overcome tumor stemness and bortezomib resistance in multiple myeloma. Cancer Lett. 520, 307–320.
Yi, Y.S., Kim, H.G., Kim, J.H., Yang, W.S., Kim, E., Jeong, D., Park, J.G., Aziz, N., Kim, S., Parameswaran, N., Cho, J.Y., 2021b. Syk-MyD88 Axis is a critical determinant of inflammatory-response in activated macrophages. Front. Immunol. 12, 767366.
Yoon, S., Kim, H., 2006. Donguibogam. Donguibogam Publishing Company, Seoul, pp. 297–2189.
Zare, A., Petrova, A., Agoumi, M., Amstrong, H., Bigras, G., Tonkin, K., Wine, E., Baksh, S., 2018. RIPK2: new elements in modulating inflammatory breast cancer pathogenesis. Cancers 10.